

Topological transitions in the presence of quenched uncorrelated disorder

Claudio Bonati¹ and Ettore Vicari²

¹*Dipartimento di Fisica dell'Università di Pisa and INFN Sezione di Pisa, Largo Pontecorvo 3, I-56127 Pisa, Italy*

²*Dipartimento di Fisica dell'Università di Pisa, Largo Pontecorvo 3, I-56127 Pisa, Italy*

(Dated: January 21, 2026)

We address issues related to the presence of defects at topological transitions, in particular when defects are modeled in terms of further variables associated with a quenched disorder, corresponding to the limit in which the defect dynamics is very slow. As a paradigmatic model, we consider the three-dimensional lattice \mathbb{Z}_2 gauge model in the presence of quenched uncorrelated disorder associated with the plaquettes of the lattice, whose topological transitions are characterized by the absence of a local order parameter. We study the critical behaviors in the presence of weak disorder. We show that they belong to a new topological universality class, different from that of the lattice \mathbb{Z}_2 gauge models without disorder, in agreement with the Harris criterium for the relevance of uncorrelated quenched disorder when the pure system undergoes a continuous transition with positive specific-heat critical exponent.

I. INTRODUCTION

Statistical systems with quenched disorder, modeling the presence of defects subject to a slow dynamics, generally develops peculiar critical phenomena associated with new universality classes with respect to pure systems, such as transitions to glassy phases. Phase transitions and critical behaviors in disordered systems have been mostly studied within lattice spin models with various realizations of local disorder, in particular with types of disorder preserving the symmetry of the pure system, such as random-bond and random-site disorder (random-field disorder instead generally breaks the global symmetry), and spatially uncorrelated probability distributions of the quenched variables, see, e.g., Refs. [1–38].

While a large amount of disorder may lead to glassy phases and glassy critical behaviors in three-dimensional (3D) spin systems, ferromagnetic transitions may still occur for sufficiently weak disorder. However, even though the quenched disorder does not change the symmetry-breaking pattern, the universality class of the critical behavior may differ from that of the ferromagnetic transition of the pure system. According to the Harris criterium [3], which applies to a spatially-uncorrelated quenched disorder that is effectively coupled to the energy density, ferromagnetic transitions in the presence of weak disorder may develop a new universality class when the specific-heat exponent α of the pure transition is positive, as it happens in 3D random-bond and random-site Ising systems [1, 2, 6, 7]. On the other hand, if the pure-system continuous transition has a negative specific-heat exponent, then its universality class turns out to be stable with respect to weak disorder, as it happens in 3D random-bond $O(N)$ vector models for any $N \geq 2$, such as the XY and Heisenberg spin models [39], corresponding to $N = 2$ and $N = 3$ respectively. Moreover, with increasing disorder, spin systems may develop peculiar multicritical behaviors along the so-called Nishimori line [2, 5, 8, 27, 32, 33], and then transitions to glassy phases, see, e.g., Refs. [13, 15–28, 30].

The effects of quenched disorder have been much less investigated at topological transitions, such as those occurring in systems with gauge symmetries, without a local order parameter driving the transition [40–43]. A paradigmatic model for systems undergoing finite-temperature topological transitions is provided by the 3D lattice \mathbb{Z}_2 gauge model [40, 41], whose confinement-deconfinement transition is not driven by a local order parameter but by the nonlocal order parameter associated with the area/perimeter law of the Wilson loops [40, 41]. 3D lattice \mathbb{Z}_2 gauge models have been also considered in the presence of local spatially-uncorrelated quenched disorder associated with each plaquette of the lattice [44, 45] (denoted by RPGM in the following), i.e., with randomly chosen plaquettes having couplings with the *wrong* (negative instead of positive) sign. The RPGM was originally introduced in relation to the theory of the quantum error correction. However, it also provides a paradigmatic example of systems undergoing topological transitions in the presence of disorder. Some results on its temperature-disorder phase diagram were reported in Refs. [45, 46], but the critical behavior at the transition lines has never been analyzed. Therefore the characterization of the universality classes of its topological transitions in the presence of quenched disorder is still an open issue.

In this paper we investigate the effects of disorder at topological transitions, focusing on the paradigmatic 3D RPGM. We recall that the pure 3D lattice \mathbb{Z}_2 gauge model is related to the standard 3D Ising model by a duality relation [40, 47], thus they share the same length-scaling critical exponent $\nu_{\mathcal{T}} \approx 0.630$ [39], which implies that the specific-heat exponent is positive, $\alpha_{\mathcal{T}} \approx 0.110$. We present a numerical analysis of the critical behaviors of the 3D lattice \mathbb{Z}_2 gauge model for weak disorder, which is made difficult by the fact that its topological transitions do not have gauge-invariant local order parameters. We thus study the critical behaviors of this system by focusing on the scaling behavior of the gauge-invariant energy cumulants. The numerical results show that the quenched disorder destabilizes the pure-system topolog-

ical transition, confirming the Harris criterium. Indeed, we observe critical behaviors belonging to another universality class with $\nu = 0.82(2)$, which is significantly larger than the Ising length-scale exponent $\nu_I \approx 0.630$ in the absence of disorder (and also any universality class of Ising systems with quenched disorder). In the final part of the paper we also briefly discuss generalizations of the RPGM, considering generic 3D lattice \mathbb{Z}_N gauge models with weak disorder.

The paper is organized as follows: in Sec. II we introduce the RPGM and discuss some properties of its phase diagram, then in Sec. III we investigate the critical behavior of this model in the regime of weak disorder, providing a quite accurate estimate of the corresponding critical exponent ν . Finally, in Sec. IV we report our conclusions and discuss some generalizations of the RPGM.

II. THE MODEL

In the statistical RPGM, i.e., a 3D lattice \mathbb{Z}_2 gauge model with uncorrelated quenched disorder associated with the plaquettes, spin variables $\sigma_{\mathbf{x},\mu} = \pm 1$ are associated with the links (starting from site \mathbf{x} in the positive μ direction, $\mu = 1, 2, 3$) of a cubic lattice of size L , and quenched disorder variables $w_{\mathbf{x},\mu\nu} = \pm 1$ are associated with the plaquettes identified by the site \mathbf{x} and the directions $\mu > \nu$. Its Hamiltonian reads [40, 44, 45]

$$H = -K \mathcal{H}, \quad \mathcal{H} = \sum_{\mathbf{x}, \mu > \nu} w_{\mathbf{x},\mu\nu} \Pi_{\mathbf{x},\mu\nu}, \quad (1)$$

where K is the gauge coupling, $\Pi_{\mathbf{x},\mu\nu}$ with $\mu > \nu$ is the plaquette operator

$$\Pi_{\mathbf{x},\mu\nu} = \sigma_{\mathbf{x},\mu} \sigma_{\mathbf{x}+\hat{\mu},\nu} \sigma_{\mathbf{x}+\hat{\nu},\mu} \sigma_{\mathbf{x},\nu}, \quad (2)$$

$\hat{\mu}$ indicates the unit vector along the direction μ and periodic boundary conditions are used on the lattice. The quenched disorder variables $w_{\mathbf{x},\mu\nu}$ ($\mu > \nu$) are spatially uncorrelated, and each disorder configuration is chosen according to the probability distribution

$$P_w(q) = \prod_{\mathbf{x}, \mu > \nu} \left[(1-q) \delta(w_{\mathbf{x},\mu\nu} - 1) + q \delta(w_{\mathbf{x},\mu\nu} + 1) \right], \quad (3)$$

where $0 \leq q \leq 1$ is a global parameter. Therefore, q is the probability of getting an extra minus sign in the Hamiltonian weight of the plaquette. The free-energy density of the RPGM is obtained by averaging over disorder configurations:

$$F(K) = \frac{1}{V} \sum_{\{\mathbf{w}\}} P_w(q) \ln Z_w(K), \quad (4)$$

$$Z_w(K) = \sum_{\{\sigma\}} e^{-H/T}, \quad V = L^3,$$

where $\{\mathbf{w}\}$ and $\{\sigma\}$ indicate disorder and spin configurations respectively. Without loss of generality, in the

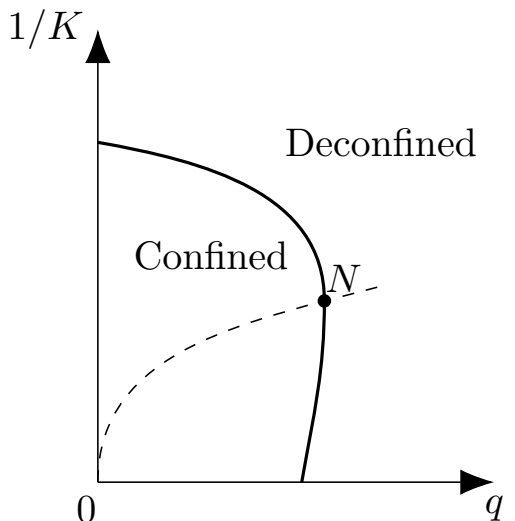


FIG. 1: The expected phase diagram of the 3D RPGM, see Refs. [45, 46]. The continuous line separates the deconfined phase, at small K^{-1} and q , from the confined phase, while the dashed line denotes the Nishimori line. The black dot N represents the point where the deconfinement transition line intersects the Nishimori line, and the value of q at this point is denoted by q_N in the main text.

following we fix $T = 1$. Therefore, the relevant phase diagram of the lattice \mathbb{Z}_2 gauge model with uniform spatially uncorrelated disorder should be studied in the q - K plane.

In the absence of disorder, which corresponds to the model in Eq. (1) for $q = 0$, the 3D lattice \mathbb{Z}_2 -gauge model undergoes a continuous topological transition at a finite value of K [40–43], $K_c(q = 0) = 0.761413292(11)$, separating the high- K deconfined phase from the low- K confined phase. This transition is topological, as it is not driven by a local order parameter. The behavior of the nonlocal Wilson loop W_C , defined as the product of the link variables along a closed contour C within a plane, provides a nonlocal order parameter for the transition [40, 41]. Indeed, its size dependence for large contours changes at K_c , from an area law $W_C \sim \exp(-c_a A_C)$ for small values of K , where A_C is the area enclosed by the contour C and $c_a > 0$ is the so called string tension, to a perimeter law $W_C \sim \exp(-c_p P_C)$ for large values of K , where P_C is the perimeter of the contour C and $c_p > 0$ is a constant. The topological transition of the 3D lattice \mathbb{Z}_2 gauge model can be related to the continuous transition of the standard 3D Ising model, because a nonlocal duality mapping relates the partition functions of the two models [40, 47]. Duality implies that thermal observables have the same critical behavior in the two models and, in particular, the correlation-length exponent ν is the same. The most accurate estimate for the 3D Ising universality class is $\nu_I = 0.629971(4)$ [48], see

also Refs. [39, 49–54] for other results.¹

The phase diagram for $q > 0$ has been discussed in Refs. [45, 46]. A sketch of the q - K^{-1} phase diagram is shown in Fig. 1. It shows notable analogies with the phase diagrams of the random-bond Ising and random-phase XY models, see, e.g., Refs. [5, 8, 15, 27, 29–34]. The deconfined phase at sufficiently large values of K is expected to extend to nonzero values of q , and it is separated from the confined phase by a transition line, which starts from the critical point along the $q = 0$ line. The so-called Nishimori line [2, 5], where K and q satisfy the relation [45]

$$e^{-2K} = \frac{q}{1-q}, \quad (5)$$

show an enhanced symmetry, which allows us to derive a number of exact relations [45]. In particular, the maximum value of q showing a deconfined phase corresponds to the location q_N of the topological confining-deconfining transition along the Nishimori line. Ref. [46] reported the estimate $q_N \approx 0.033$. The transition line below the Nishimori critical point is likely slightly reentrant, as it also occurs in random-bond Ising models, see, e.g., Ref. [30, 34]. There is no evidence of the existence of further gauge glassy phase for $q > q_N$, as characterized in Ref. [45], although its presence cannot be excluded yet. Therefore, the phase diagram should be similar to that of the 2D random-bond Ising model [5, 31, 34, 35, 45] with the ferromagnetic and paramagnetic phases replaced by the deconfined and confined phases, as sketched in Fig. 1. In this work we focus on the critical properties at the confined-deconfined topological transition for small disorder parameter q , up to the critical point N along the Nishimori line.

According to the Harris criterium [3], spatially uncorrelated quenched disorder coupled to the energy density of the system provides a relevant perturbation at the fixed points corresponding to the critical behavior of pure systems with positive specific-heat exponent. This is for example the case of the 3D random-bond Ising model where the specific-heat exponent of the pure Ising transition is $\alpha_{\mathcal{I}} = 2 - 3\nu_{\mathcal{I}} \approx 0.110$. In this case the critical behavior at the ferromagnetic transitions in the presence of spatially uncorrelated disorder belong to a different universality class, the so called randomly-dilute Ising (RDI) universality class, whose length-scale critical exponent is $\nu_{\text{rdi}} = 0.683(2)$ [6, 7, 65], and the corresponding specific-heat exponent is negative, $\alpha_{\text{rdi}} = 2 - 3\nu_{\text{rdi}} = -0.049(6)$. An analogous change of universality class occurs also in the 3D RPGM for $q > 0$. Indeed, also in this case we have spatially uncorrelated quenched variables coupled to the energy density, which corresponds to the plaquette term

in lattice \mathbb{Z}_2 gauge models. Therefore, the universality class of the disordered topological transitions is expected to differ from that of the pure model at $q = 0$. Note also that there is no reason to expect that such transition belongs to the RDI universality class of disordered spin systems, since the duality mapping with the Ising model is lost in the presence of disorder.

We finally mention that the results reported in Ref. [45, 46] along the confining-deconfining transition do not give hints of the universality class of the critical behavior for weak disorder, and in particular of the corresponding critical exponent ν .

III. NUMERICAL METHODS AND RESULTS

Topological transitions are notoriously difficult to investigate, due to the absence of local order parameters. It might seem that the natural strategy for investigating the topological transitions of lattice \mathbb{Z}_2 gauge models is to study the area or perimeter law behavior of large Wilson loops, as done in [46]. Such a strategy is however effective only if we want to investigate the phase structure of the model, and it becomes more and more inefficient as we approach a continuous phase transition. It indeed requires the use of very large lattices to estimate the (vanishing at the transition) string tension from the large distance behavior of Wilson loops. In our numerical study we follow a more convenient numerical approach, which lends itself for a finite-size scaling (FSS) analysis at the critical point.

We study the FSS behavior of the gauge-invariant energy cumulants, normalized by the lattice volume and averaged over disorder. These quantities, which will be denoted by B_k in the following, are the intensive quantities defined by

$$B_k = \left(\frac{\partial}{\partial K} \right)^k F(K) = \frac{1}{V} \sum_{\{w\}} P_w(q) \left(\frac{\partial}{\partial K} \right)^k \ln Z_w(K). \quad (6)$$

The cumulants can be related (for $k > 1$) to the central moments of the energy defined for each disorder realization by

$$m_k = \langle (\mathcal{H} - \langle \mathcal{H} \rangle)^k \rangle, \quad (7)$$

where \mathcal{H} is defined in Eq. (1), and the statistical average $\langle \cdot \rangle$ is taken over the spin variables at fixed disorder configuration. One can easily see that B_1 is proportional to energy density, i.e.,

$$B_1 = \frac{1}{V} [\langle \mathcal{H} \rangle]_w, \quad (8)$$

where the square brackets $[\cdot]_w$ indicate the average over the quenched disorder, while the second and third cumu-

¹ The universal features of the topological confinement-deconfinement transitions of 3D lattice \mathbb{Z}_N models have been investigated in several works, see, e.g., Refs. [40, 43, 55–64].

lants are given by

$$B_k = \frac{1}{V} [m_k]_w \quad \text{for } k = 2, 3. \quad (9)$$

In particular, B_2 is proportional to the specific heat. The relation between cumulants and central moments becomes more complicated for higher cumulants, for example

$$B_4 = \frac{1}{V} [m_4 - 3m_2^2]_w. \quad (10)$$

The energy cumulants are very useful to characterize topological transitions in which no local gauge-invariant order parameter is present (see, e.g., Refs. [66–70]), since for fixed q they are expected to show the FSS behavior [66, 69]

$$B_k(K, L) \approx L^{k/\nu-3} \mathcal{B}_k(X) + b_k, \quad (11)$$

$$X = (K - K_c)L^{1/\nu}, \quad (12)$$

where the constants b_k represent the analytic background [39, 69], and we neglect $O(L^{-\omega})$ scaling corrections to the leading scaling behavior [the exponent $\omega > 0$ is generally associated with the leading irrelevant renormalization group (RG) perturbation at the fixed point [39], for example $\omega \approx 0.8$ at the standard Ising transition, i.e., for $q = 0$]. The scaling functions $\mathcal{B}_k(X)$ are universal apart from a multiplicative factor and a normalization of the argument, however they generally depend on the boundary conditions adopted.

It is important to stress that background term b_k in Eq. (11) turns out to be subleading with respect to the scaling term only when $k - 3\nu > 0$, thus for $k \geq 2$ when the specific-heat exponent is positive, i.e., $\alpha = 2 - 3\nu > 0$, which is the case for $q = 0$. If instead $\alpha < 0$, which is the case expected along the confining-deconfining transition line for $q > 0$ due to Harris criterium, higher cumulants are needed to identify the scaling behavior, with minimum value of k depending on the critical exponent ν . Note however that higher cumulants also become more noisy, so it is typically convenient to use the cumulant corresponding to the smallest value of k such that $k - 3\nu > 0$.

To characterize the critical behavior of the RPGM for weak disorder we present a numerical FSS analysis for $q = 0.015$, which according to the results of Ref. [46] should be sufficiently small for the system to develop a finite-temperature confining-deconfining transition. We thus perform simulations for $q = 0.015$ and several values of K , for lattice sizes up to $L = 32$. We use $O(10^3)$ noise samples and for each noise realization we carry out 2×10^5 Metropolis updates of the whole lattice, discarding one quarter (half, for the largest lattices) of them as thermalization. Moreover, three independent simulations have been carried out for each noise realization, in order to obtain unbiased estimates of the first three cumulants of the energy (see [7] for a discussion of this point).

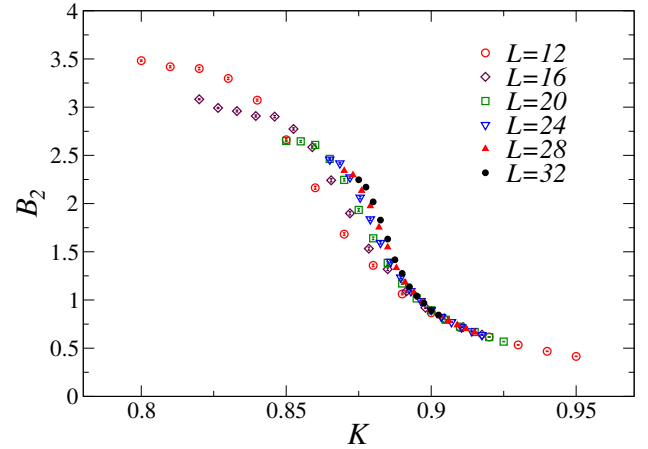


FIG. 2: Data for the second cumulant B_2 , proportional to the specific heat, across the topological transition for $q = 0.015$.

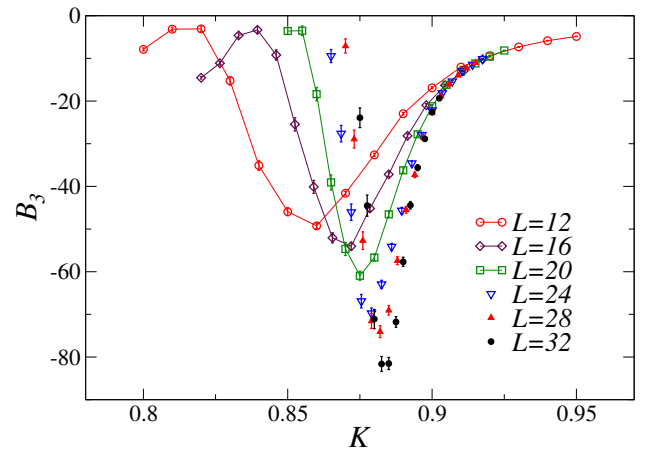


FIG. 3: Data for the third cumulant B_3 for $q = 0.015$, across the topological transition around $K \approx 0.89$. Continuous lines for $L = 12, 16, 20$ are drawn just to guide the eye.

The numerical results obtained for the second cumulant B_2 , corresponding to the specific heat, are shown in Fig. 2. They do not appear to diverge with increasing L , implying that $\alpha < 0$, consistently with the expectations coming from Harris criterium. In Fig. 3 we report data for the third cumulant B_3 , which is the first cumulant to display an apparently divergent behavior at the transition. To estimate K_c and ν we performed several fits using the FSS relation in Eq. (11), with a polynomial approximation of $\mathcal{B}_k(X)$ and taking also into account scaling corrections, i.e., using the functional form

$$B_3(K, L) = L^{3/\nu-3} \left(\sum_{i=0}^{n_l} a_i X^i + L^{-\kappa} \sum_{i=0}^{n_s} b_i X^i \right). \quad (13)$$

If $\omega < 3/\nu - 3$ then $\kappa = \omega$ and the $O(L^{-\kappa})$ term parametrizes the correction due to the leading irrelevant perturbation [not explicitly written in Eq. (11)]. If instead $\omega > 3/\nu - 3$ then $\kappa = 3/\nu - 3$ and the $O(L^{-\kappa})$ term takes into account the analytic background in Eq. (11),

L_{\min}	fit range	scal.	corr.	K_c	ν	χ^2/dof
20	[-1.5,1]	no		0.89436(33)	0.8162(56)	69/42
24	[-1.5,1]	no		0.89442(53)	0.826(10)	32/28
20	[-1,1]	no		0.89393(50)	0.8102(76)	65/35
24	[-1,1]	no		0.89396(82)	0.821(14)	27/21
20	[-0.5,0.5]	no		0.8933(17)	0.811(31)	12/11
24	[-0.5,0.5]	no		0.8919(23)	0.782(46)	12/9
12	[-1.5,1]	fit κ		0.89371(29)	0.8129(54)	67/58
16	[-1.5,1]	fit κ		0.89414(63)	0.822(15)	46/46
16	[-1.5,1]	$\kappa = 0.5$		0.89389(42)	0.802(10)	70/55
20	[-1.5,1]	$\kappa = 0.5$		0.89406(67)	0.792(21)	36/36
16	[-0.5,0.5]	$\kappa = 0.5$		0.89370(98)	0.827(14)	41/28
20	[-0.5,0.5]	$\kappa = 0.5$		0.8927(21)	0.813(32)	18/17
16	[-1.5,1]	$\kappa = 1.0$		0.89382(40)	0.804(10)	69/55
20	[-1.5,1]	$\kappa = 1.0$		0.89301(69)	0.800(20)	46/38
16	[-0.5,0.5]	$\kappa = 1.0$		0.89298(91)	0.817(13)	32/28
20	[-0.5,0.5]	$\kappa = 1.0$		0.8932(20)	0.820(30)	16/16

TABLE I: Some of the fits performed to estimate K_c and ν for $q = 0.015$. L_{\min} denotes the smallest value of the lattice size considered in the fit, and the fit range refers to the values of X , cf. Eq. (12), self-consistently used in the fit. Scaling corrections have been either totally neglected, or taken into account by fixing the reported value of κ (see text), or taken into account by leaving κ as a free parameter in the fit. In the last case, however, the value of κ could not be reliably estimated due to large statistical uncertainties. The errors on the various results are only statistical.

and in this case $n_s = 0$ should be used.

The outcomes of some of these fits are reported in Table I, and our optimal estimates are

$$K_c = 0.8940(8), \quad \nu = 0.82(2). \quad (14)$$

The uncertainty on these estimates is dominated by the systematic errors, which have been estimated by varying the degree of the polynomial approximations (which has in fact a very mild effect), by varying the fit range, by systematically discarding the data coming from the smaller lattices in the fit to check the effects of scaling corrections, and by adding some scaling corrections, see Table I. In Fig. 4 we show the resulting FSS of B_3 when using our optimal estimates reported in Eq. (14), showing the good quality of the collapse of the data.²

A reasonable hypothesis is that the value $\nu = 0.82(2)$ of the length-scale critical exponent characterizes the critical behavior along the whole transition line up to to the Nishimori point. Note that the value of ν that we have obtained is significantly larger than the Ising exponent

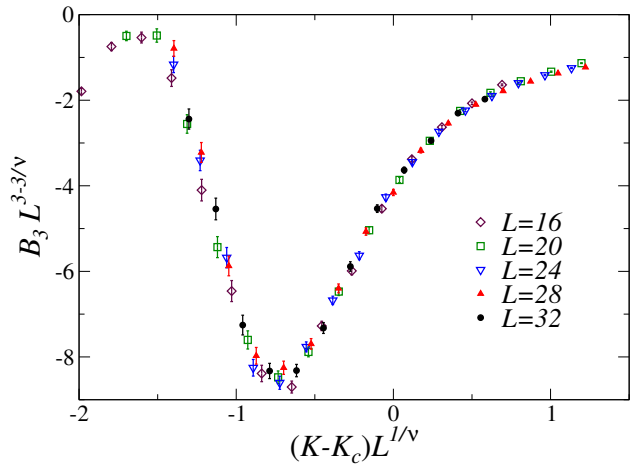


FIG. 4: Scaling of third cumulant B_3 for $q = 0.015$, obtained by plotting $L^{3-3/\nu} B_3$ versus $(K - K_c) L^{1/\nu}$ with our optimal estimates $K_c = 0.8940$ and $\nu = 0.82$.

$\nu_{\mathcal{I}} \approx 0.630$ in the absence of disorder. Moreover, the corresponding value of the specific-heat exponent is negative, $\alpha = 2 - 3\nu = -0.46(6)$, as expected by the Harris criterium. We also note that the value ν obtained by our numerical analysis, cf. Eq. (14), implies that the background term in the FSS relation in Eq. (11) for the third cumulant is suppressed as $O(L^{-(3/\nu-3)})$ with $3/\nu - 3 = 0.66(7)$. Further $O(L^{-\omega})$ scaling corrections arising from the leading irrelevant RG perturbation are also expected, however the available data are not sufficiently precise to reliably estimate the value of ω .

To verify that the universality class of the transitions does not change along the confinement-deconfinement transition line for weak disorder, we now present results obtained by fixing $K = 1.0$, performing a scan in q . Also in this case the specific heat does not display a divergent behavior, and the first seemingly divergent cumulant is the third one, see Fig. 5. To extract the critical properties from these data we can follow the same strategy already adopted for the transition at $q = 0.015$, the only difference being that the scaling variable to be used in Eq. (11) is now

$$X = (q - q_c) L^{1/\nu} \quad (15)$$

instead of Eq. (12). The final result of this analysis are the estimates

$$q_c = 0.0219(3), \quad \nu = 0.84(8), \quad (16)$$

where the reported errors are largely dominated by systematic errors. The estimated value of the critical exponent ν is fully consistent with the one obtained previously, see Eq. (14), although significantly less accurate.

In Fig. 6 we show the scaling plot obtained by rescaling B_3 data using the optimal value q_c in Eq. (16) and the critical exponent $\nu = 0.82$ obtained at fixed $q = 0.015$. The results are substantially consistent, however we note

² The estimate of K_c that we report in Eq. (14) is significantly more accurate than the estimate reported in Ref. [46], which was $K_c \approx 0.866$, somehow obtained from the specific-heat data for $L = 24$ at $q = 0.015$.

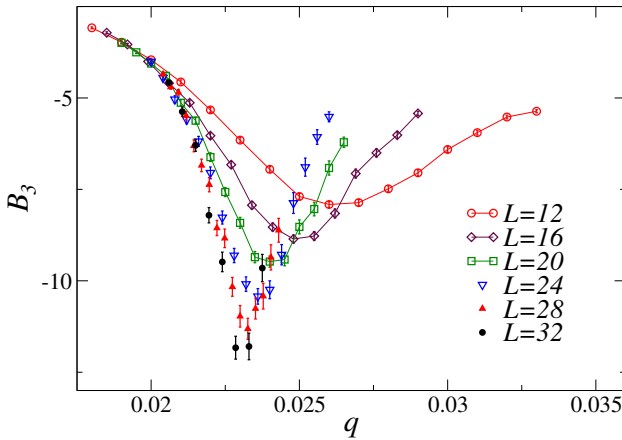


FIG. 5: Data for the third cumulant B_3 for $K = 1$, across the topological transition around $q \approx 0.022$. Continuous lines for $L = 12, 16, 20$ are drawn just to guide the eye.

that scaling corrections are much larger than the data at fixed $q = 0.015$, see Fig. 4. This slower approach to the asymptotic critical behavior may be explained by two different reasons. The first possible cause is that we changed the variable that is kept fixed in the scan (q in the previous case, K now), and if the confinement-deconfinement transition line is almost parallel to the q axis for $K \approx 1$ this results in a significant increase of scaling corrections. The other possible cause is that we are getting closer to the Nishimori point, and crossover effects can thus be present on small lattices. The qualitative behaviors of the B_3 curves obtained for $K = 1$ and $q = 0.015$ is the same, however the presence of large scaling corrections for $K = 1$ makes it impossible to achieve a robust quantitative check that the asymptotic scaling curves associated with B_3 , cf. Eq. (11), are the same up to rescaling coefficients in the two cases.

In conclusion, we believe that our results provide a quite robust evidence that the topological transitions of the 3D lattice \mathbb{Z}_2 gauge model changes universality class in the presence of quenched uncorrelated disorder associated with the plaquette. Moreover, we note that the exponent ν of this new universality class significantly differs from that of the ferromagnetic transitions in 3D random-bond Ising models, for which [6] $\nu_{\text{rdi}} = 0.683(2)$.

IV. CONCLUSIONS

We have investigated the effects of quenched disorder at topological transitions, focusing on the 3D \mathbb{Z}_2 gauge model in the presence of an uncorrelated quenched disorder associated with the plaquettes of the lattice (RPGM). This is paradigmatic model for systems undergoing finite-temperature topological transitions [40–43], indeed its confinement-deconfinement transitions are not driven by any local order parameter. We report a numerical analysis of their critical behaviors for weak disorder, and

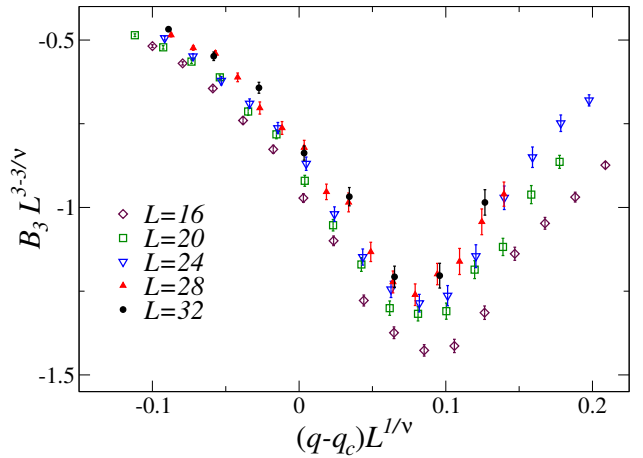


FIG. 6: Scaling of third cumulant B_3 for $K = 1$, obtained by plotting $L^{3-3/\nu} B_3$ versus $(K - K_c) L^{1/\nu}$ using our optimal estimates $K_c = 0.0219$ and the value $\nu = 0.82$ obtained in the $q = 0.015$ case.

for this purpose we focus on the scaling behavior of the gauge-invariant energy cumulants defined in Eq. (6). The numerical investigation has been carried out using the binomial distribution for disorder variables, but it is natural to guess that the universality class of the results is independent of the disorder distribution, as it happens for the Ising model with quenched disorder, see, e.g., Ref. [7].

We show that the topological transitions of the 3D RPGM belong to a new topological universality class, different from that of the pure system, in agreement with the Harris criterium for the relevance of uncorrelated quenched disorder when the pure system undergoes a continuous transition with positive specific-heat critical exponent. Indeed, the critical behavior in the presence of weak disorder turns out to be characterized by the length-scale critical exponent $\nu = 0.82(2)$, which is significantly larger than the Ising length-scale critical exponent $\nu_{\text{Ising}} \approx 0.630$ in the absence of disorder.

The same universality class is expected to describe all the transitions happening for $q < q_N$ and $K < K_N$, where (q_N, K_N) is the intersection point of the deconfinement transition line and the Nishimori line, see Fig. 1. At this intersection point the RPGM is expected to develop a peculiar multicritical behavior, characterized by two relevant RG perturbations with RG dimensions $y_1 > y_2 > 0$. Analogously to the multicritical behavior at the Nishimori point of the 2D and 3D random-bond Ising models [5, 8, 32, 33], we expect that the multicritical behavior of RPGM is characterized by two relevant RG perturbations associated with the scaling fields $u_1 = q - q_N$, which runs parallel to the transition line at the Nishimori point, and $u_2 = \tanh K + 2q - 1$, with corresponding RG dimensions y_1 and y_2 respectively, so that $y_1 > y_2 > 0$. Unfortunately, this multicritical behavior cannot be investigated using the techniques adopted in the present study. This is due to the fact that the energy density, and all the energy cumulants, along the Nishimori line

are analytic functions, indeed the exact result [45]

$$\frac{1}{V} [\langle \mathcal{H} \rangle]_w = 3 - 6q \quad (17)$$

holds along the Nishimori line (5) (see also analogous behaviors [2, 5] for the random-bond Ising model). Therefore, the scaling part of the cumulants vanishes along the Nishimori. We also note that the critical behaviors along the deconfinement-confinement transition line below the Nishimori point, see Fig. 1, is expected to belong to a different universality class, as it occurs for other systems with quenched disorder, see, e.g., Refs. [27, 30, 34].

We finally discuss possible extensions of this study to generic lattice \mathbb{Z}_N gauge models with $N > 2$ in the presence of quenched disorder associated with the plaquette, which are simply obtained by replacing the \mathbb{Z}_2 link variable $\sigma_{\mathbf{x},\nu}$ in the plaquette operator (2) with $\lambda_{\mathbf{x},\nu} = \exp(i2\pi n_{\mathbf{x},\nu}/N)$ with $n_{\mathbf{x},\nu} = 0, 1, \dots, N - 1$, and using the real part of the plaquette operator in the Hamiltonian (for $N = 2$ we recover the \mathbb{Z}_2 gauge model). We recall that, in the absence of quenched disorder, therefore for $q = 0$ in Eq. (3), 3D lattice \mathbb{Z}_N gauge models undergo finite-temperature topological transitions for any N . For $N > 4$ the transitions are continuous and belong to the inverted XY (IXY) universality class [43, 59, 66, 71]. For $N = 4$ the transition is continuous and belongs to the Ising universality class because its partition functions can be written as the square of the partition function of the lattice \mathbb{Z}_2 gauge model (note however that this

holds only for the specific plaquette Hamiltonian that we consider [43]). Finally the transition is first order for $N = 3$. Therefore, since the specific-heat critical exponent of the IXY universality class is negative [39, 43] (it is equal to that of the duality related XY universality class, $\alpha \approx -0.015$), according to the Harris criterium we expect that a weak quenched disorder is irrelevant for $N > 4$, and the topological transitions still belong to the IXY universality class. On the other hand, the quenched disorder must be relevant for $N = 4$ if the plaquette action is used, because its specific heat exponent is positive. Indeed, analogously to the pure case [69, 72], one can easily prove that for each disorder configuration the partition function of $N = 4$ model satisfies the identity

$$Z_{N=4,w}(K) = Z_{N=2,w}(K/2)^2. \quad (18)$$

The corresponding free-energy density (4) in the presence of disorder is thus equivalent to that of the 3D lattice \mathbb{Z}_2 gauge model. Therefore, we expect to observe continuous transitions analogous to those found in the 3D lattice \mathbb{Z}_2 gauge model with quenched disorder, apart from a trivial change of the coupling K according to the identity (18). On the other hand, the situation is less clear for $N = 3$: the first-order transitions of pure systems are generically expected to be smoothed by the quenched disorder (see, e.g., [73]), and may give rise to continuous transitions belonging to a new universality class.

[1] S.-k. Ma, *Modern theory of critical phenomena*, (Benjamin/Cummings, Reading, MA, 1976).

[2] H. Nishimori, *Statistical Physics of Spin Glasses and Information Processing: An Introduction*, Oxford University Press, Oxford, 2001.

[3] A. B. Harris, Journal of Physics C: Solid State Physics Effect of random defects on the critical behaviour of Ising models, *J. Phys. C: Solid State Phys.* **7**, 1671 (1974).

[4] S. F. Edwards and P. W. Anderson, Theory of spin glasses, *J. Phys. F: Met. Phys.* **5**, 965 (1975).

[5] H. Nishimori, Internal Energy, Specific Heat and Correlation Function of the Bond-Random Ising Model, *Prog. Theor. Phys.* **66**, 1169 (1981).

[6] M. Hasenbusch, F. Parisen Toldin, A. Pelissetto, and E. Vicari, The critical behavior of the 3D $\pm J$ Ising model at the ferromagnetic transition line, *Phys. Rev. B* **76**, 094402 (2007).

[7] M. Hasenbusch, F. Parisen Toldin, A. Pelissetto, and E. Vicari, Universality class of 3D site-diluted and bond-diluted Ising systems, *J. Stat. Mech.: Theory Exp.* (2007) P02016.

[8] M. Hasenbusch, F. Parisen Toldin, A. Pelissetto, and E. Vicari, Magnetic-glassy multicritical behavior of 3D $\pm J$ Ising model, *Phys. Rev. B* **76**, 184202 (2007).

[9] M. Palassini and S. Caracciolo, Universal Finite-Size Scaling Functions in the 3D Ising Spin Glass, *Phys. Rev. Lett.* **82**, 5128 (1999).

[10] H. G. Ballesteros, A. Cruz, L. A. Fernández, V. Martín-Mayor, J. Pech, J. J. Ruiz-Lorenzo, A. Tarancón, P. Téllez, C. L. Ullod, and C. Ungil, Critical behavior of the three-dimensional Ising spin glass, *Phys. Rev. B* **62**, 14237 (2000).

[11] F. Krzakala and O. C. Martin, Absence of an Equilibrium Ferromagnetic Spin-Glass Phase in Three Dimensions, *Phys. Rev. Lett.* **89**, 267202 (2002).

[12] N. Kawashima and H. Rieger, in *Frustrated Spin Systems*, edited by H.T. Diep (World Scientific, Singapore, 2004); cond-mat/0312432.

[13] H. G. Katzgraber, M. Körner, and A. P. Young, Universality in three-dimensional Ising spin glasses: A Monte Carlo study, *Phys. Rev. B* **73**, 224432 (2006).

[14] T. Jörg, Critical behavior of the three-dimensional bond-diluted Ising spin glass: Finite-size scaling functions and universality, *Phys. Rev. B* **73**, 224431 (2006).

[15] M. Hasenbusch, A. Pelissetto, and E. Vicari, Critical behavior of three-dimensional Ising spin glass models, *Phys. Rev. B* **78**, 214205 (2008); The critical behavior of 3D Ising spin glass models: universality and scaling corrections, *J. Stat. Mech.: Theory Exp.* L02001 (2008).

[16] A. Billoire, L. A. Fernandez, A. Maiorano, E. Marinari, V. Martin-Mayor, and D. Yllanes, Finite-size scaling analysis of the distributions of pseudo-critical temperatures in spin glasses, *J. Stat. Mech.* (2011) P10019.

[17] Janus Collaboration, M. Baity-Jesi, R. A. Baños, A.

Cruz, L. A. Fernandez, J. M. Gil-Narvion, A. Gordillo-Guerrero, D. Iñiguez, A. Maiorano, F. Mantovani, E. Marinari, V. Martin-Mayor, J. Monforte-Garcia, A. Muñoz Sudupe, D. Navarro, G. Parisi, S. Perez-Gaviro, M. Pivanti, F. Ricci-Tersenghi, J. J. Ruiz-Lorenzo, S. F. Schifano, B. Seoane, A. Tarancón, R. Tripiccione, and D. Yllanes, Critical parameters of the three-dimensional Ising spin glass, *Phys. Rev. B* **88**, 224416 (2013).

[18] M. Lulli, G. Parisi, and A. Pelissetto, Out-of-equilibrium finite-size method for critical behavior analyses, *Phys. Rev. E* **93**, 032126 (2016).

[19] E. Granato, Critical behavior and driven Monte Carlo dynamics of the XY spin glass in the phase representation, *Phys. Rev. B* **69**, 144203 (2004).

[20] M. Matsumoto, K. Hukushima, and H. Takayama, Dynamical Critical Phenomena in three-dimensional Heisenberg Spin Glasses, *Phys. Rev. B* **66**, 104404 (2002).

[21] M. Picco and F. Ritort, Dynamical AC study of the critical behavior in Heisenberg spin glasses *Phys. Rev. B* **71**, 100406 (2005).

[22] L. W. Lee and A. P. Young, Large-scale Monte Carlo simulations of the isotropic three-dimensional Heisenberg spin glass, *Phys. Rev. B* **76**, 024405 (2007).

[23] D. X. Viet and H. Kawamura, Numerical evidence of the spin-chirality decoupling in the three-dimensional Heisenberg spin glass, *Phys. Rev. Lett.* **102**, 027202 (2009); Monte Carlo studies of the chiral and spin orderings of the three-dimensional Heisenberg spin glass, *Phys. Rev. B* **80**, 064418 (2009).

[24] L. A. Fernandez, V. Martin-Mayor, S. Perez-Gaviro, A. Tarancón, and A. P. Young, Phase transition in the three-dimensional Heisenberg spin glass: Finite-size scaling analysis, *Phys. Rev. B* **80**, 024422 (2009).

[25] M. Baity-Jesi, L. A. Fernandez, V. Martin-Mayor, and J. M. Sanz, Phase Transition in 3d Heisenberg Spin Glasses with Strong Random Anisotropies, through a Multi-GPU Parallelization, *Phys. Rev. B* **89**, 014202 (2014).

[26] T. Ogawa, K. Uematsu, and H. Kawamura, Monte Carlo studies of the spin-chirality decoupling in the three-dimensional Heisenberg spin glass, *Phys. Rev. B* **101**, 014434 (2020).

[27] V. Alba and E. Vicari, Temperature-disorder phase diagram of a three-dimensional gauge-glass model, *Phys. Rev. B* **83**, 094203 (2011).

[28] T. Aspelmeier, H. G. Katzgraber, D. Larson, M. A. Moore, M. Wittmann, and J. Yeo, Finite-size critical scaling in Ising spin glasses in the mean-field regime, *Phys. Rev. E* **93**, 032123 (2016).

[29] A. K. Hartmann, Ground-state behavior of the three-dimensional $\pm J$ random-bond Ising model, *Phys. Rev. B* **59**, 3617 (1999).

[30] G. Ceccarelli, A. Pelissetto, and E. Vicari, Ferromagnetic-glassy transitions in three-dimensional Ising spin glasses, *Phys. Rev. B* **84**, 134202 (2011).

[31] M. Picco, A. Honecker, and P. Pujol, Strong disorder fixed points in the two-dimensional random-bond Ising model, *J. Stat. Mech.: Theory Exp.* (2006) P09006.

[32] P. Le Doussal and A. B. Harris, Location of the Ising Spin-Glass multicritical point on Nishimori's line, *Phys. Rev. Lett.* **61**, 625 (1988).

[33] M. Hasenbusch, F. Parisen Toldin, A. Pelissetto, and E. Vicari, Multicritical Nishimori point in the phase diagram of the $\pm J$ Ising model on the square lattice, *Phys. Rev. E* **77**, 051115 (2008).

[34] F. Parisen Toldin, A. Pelissetto, and E. Vicari, Strong-disorder paramagnetic-ferromagnetic fixed point in the square-lattice $\pm J$ Ising model, *Journal of Stat. Phys.* **135**, 1039 (2009); Universality of the glassy transitions in the two-dimensional $\pm J$ Ising model, *Phys. Rev. E* **82**, 021106 (2010).

[35] L. A. Fernandez, E. Marinari, V. Martin-Mayor, G. Parisi, and J. J. Ruiz-Lorenzo, Universal critical behavior of the 2d Ising spin glass, *Phys. Rev. B* **94**, 024402 (2016).

[36] A. G. Cavaliere and A. Pelissetto, Disordered Ising model with correlated frustration, *J. Phys. A* **52**, 174002 (2019).

[37] H. Nishimori, Anomalous distribution of magnetization in an Ising spin glass with correlated disorder, *Phys. Rev. E* **110**, 064108 (2024); Instability of the ferromagnetic phase under random fields in an Ising spin glass with correlated disorder, *Phys. Rev. E* **111**, 044109 (2025).

[38] T. Vojta, Disorder in quantum many-body systems, *Annu. Rev. Condens. Matter Phys.* **10**, 233 (2019).

[39] A. Pelissetto and E. Vicari, Critical phenomena and renormalization group theory, *Phys. Rep.* **368**, 549 (2002).

[40] F. J. Wegner, Duality in generalized Ising models and phase transitions without local order parameters, *Jour. of Math. Phys.* **12**, 2259 (1971).

[41] J. Kogut, An introduction to lattice gauge theory and spin systems, *Rev. Mod. Phys.* **51**, 659 (1979).

[42] S. Sachdev, Topological order, emergent gauge fields, and Fermi surface reconstruction, *Rep. Prog. Phys.* **82**, 014001 (2019).

[43] C. Bonati, A. Pelissetto, and E. Vicari, Three-dimensional Abelian and non-Abelian gauge Higgs theories, *Phys. Rep.* **1133**, 1 (2025).

[44] E. Dennis, A. Kitaev, A. Landahl, and J. Preskill, Topological quantum memory, *J. Math. Phys.* **43**, 4452 (2002).

[45] C. Wang, J. Harrington, and J. Preskill, Confinement-Higgs transition in a disordered gauge theory and the accuracy threshold for quantum memory, *Ann. Phys.* **303**, 31 (2003).

[46] T. Ojno, G. Arakawa, I. Ichinose, and T. Matsui, Structure of the Random-Plaquette \mathbb{Z}_2 Gauge Model: Accuracy Threshold for a Toric Quantum Memory, *Nucl. Phys. B* **697**, 462 (2004).

[47] R. Savit, Duality in Field Theory and Statistical Systems, *Rev. Mod. Phys.* **52**, 453 (1980).

[48] F. Kos, D. Poland, D. Simmons-Duffin, and A. Vichi, Precision islands in the Ising and $O(N)$ models, *J. High Energy Phys. JHEP* 08 (2016) 036.

[49] M. Hasenbusch, Restoring isotropy in a three-dimensional lattice model: The Ising universality class, *Phys. Rev. B* **104**, 014426 (2021).

[50] A. M. Ferrenberg, J. Xu, and D. P. Landau, Pushing the limits of Monte Carlo simulations for the three-dimensional Ising model, *Phys. Rev. E* **97**, 043301 (2018).

[51] M. V. Kompaniets and E. Panzer, Minimally subtracted six-loop renormalization of ϕ^4 -symmetric theory and critical exponents, *Phys. Rev. D* **96**, 036016 (2017).

[52] M. Hasenbusch, Finite-size scaling study of lattice models in the three-dimensional Ising universality class, *Phys. Rev. B* **82**, 174433 (2010).

[53] M. Campostrini, A. Pelissetto, P. Rossi, and E. Vicari, 25th order high-temperature expansion results for three-dimensional Ising-like systems on the simple cubic lattice, *Phys. Rev. E* **65**, 066127 (2002).

[54] R. Guida and J. Zinn-Justin, Critical exponents of the N -vector model, *J. Phys. A* **31**, 8103 (1998).

[55] R. Balian, R. J. M. Drouffe, and C. Itzykson, Gauge Fields on a Lattice. I. General Outlook, *Phys. Rev. D* **10**, 3376 (1976).

[56] R. Ben-Av, D. Kandel, E. Katznelson, P. G. Lauwers, and S. Solomon, Critical acceleration of lattice gauge simulations. *Journal of Stat. Phys.* **58**, 125 (1990).

[57] M. Caselle, R. Fiore, F. Gliozzi, M. Hasenbusch, and P. Provero, String effects in the Wilson loop: A High precision numerical test, *Nucl. Phys. B* **486**, 245 (1997).

[58] G. Gliozzi, M. Panero, and P. Provero, Large center vortices and confinement in 3-D Z_2 gauge theory, *Phys. Rev. D* **66**, 017501 (2002).

[59] O. Borisenko, V. Chelnokov, G. Cortese, M. Gravina, A. Papa, and I. Surzhikov, Critical behavior of 3D $Z(N)$ lattice gauge theories at zero temperature, *Nucl. Phys. B* **879**, 80 (2014).

[60] N. Xu, C. Castelnovo, R. G. Melko, C. Chamon, and A. W. Sandvik, Dynamic scaling of topological ordering in classical systems, *Phys. Rev. B* **97**, 024432 (2018).

[61] R. Agrawal, L. F. Cugliandolo, L. Faoro, L. B. Ioffe, and M. Picco, The geometric phase transition of the three-dimensional Z_2 lattice gauge model, *Phys. Rev. Lett.* **135**, 120601 (2025).

[62] C. Bonati, A. Pelissetto, and E. Vicari, Critical relaxational dynamics at the continuous transitions of three-dimensional spin models with Z_2 gauge symmetry, *Phys. Rev. B* **111**, 115129 (2025).

[63] C. Bonati, H. Panagopoulos, and E. Vicari, Out-of-equilibrium critical dynamics of the three-dimensional Z_2 gauge model along critical relaxational flows, *Phys. Rev. E* **111**, 054107 (2025).

[64] C. Bonati, H. Panagopoulos, E. Vicari, Critical relaxational dynamics of three-dimensional lattice Z_N gauge models and the inverted XY universality class, *Phys. Rev. E* **112** 024125 (2025).

[65] A. Pelissetto and E. Vicari, Randomly dilute spin models: a six-loop field-theoretic study, *Phys. Rev. B* **62**, 6393 (2000).

[66] J. Smiseth, E. Smørgrav, F. S. Nogueira, J. Hove, and A. Sudbø, Phase Structure of $d = 2 + 1$ Compact Lattice Gauge Theories and the Transition from Mott Insulator to Fractionalized Insulator, *Phys. Rev. B* **67**, 205104 (2003).

[67] C. Bonati, A. Pelissetto, and E. Vicari, Higher-charge three-dimensional compact lattice Abelian-Higgs models, *Phys. Rev. E* **102**, 062151 (2020).

[68] C. Bonati, A. Pelissetto, and E. Vicari, Multicritical point of the three-dimensional Z_2 gauge Higgs model, *Phys. Rev. B* **105**, 165138 (2022).

[69] C. Bonati, A. Pelissetto, and E. Vicari, Deconfinement transitions in three-dimensional compact lattice Abelian Higgs models with multiple-charge scalar fields, *Phys. Rev. E* **109**, 044146 (2024).

[70] C. Bonati, A. Pelissetto, and E. Vicari, Diverse universality classes of the topological deconfinement transitions of three-dimensional noncompact lattice Abelian Higgs models *Phys. Rev. D* **109**, 034517 (2024).

[71] C. Bonati, A. Pelissetto, and E. Vicari, Scalar gauge-Higgs models with discrete Abelian symmetry groups, *Phys. Rev. E* **105**, 054132 (2022).

[72] C. P. Korthals Altes, Duality for $Z(N)$ Gauge Theories, *Nucl. Phys. B* **142**, 315 (1978).

[73] J. Cardy, Quenched Randomness at First-Order Transitions, *Physica A* **263**, 215 (1999).